

FINAL REPORT

(Contract No. FA5209-06-P-0213)

Program Manager: Dr. Misoon Y. Mah

**Project Title: High-temperature Ferromagnetism in Cr- and
Mn-implanted $\text{Al}_x\text{Ga}_{1-x}\text{N}$**

Report Period: 24 March 2006 -23 September 2007

Principal Investigator: Prof. Mee-Yi Ryu

**Department of Physics
Kangwon National University
192-1 Hyoja2-Dong, Chuncheon
Kangwon-Do 200-701, Korea
Phone: +82-33-250-8474
Fax: +82-33-257-9689**

Starting Date: 24 March 2006

Report Documentation Page				Form Approved OMB No. 0704-0188	
Public reporting burden for the collection of information is estimated to average 1 hour per response, including the time for reviewing instructions, searching existing data sources, gathering and maintaining the data needed, and completing and reviewing the collection of information. Send comments regarding this burden estimate or any other aspect of this collection of information, including suggestions for reducing this burden, to Washington Headquarters Services, Directorate for Information Operations and Reports, 1215 Jefferson Davis Highway, Suite 1204, Arlington VA 22202-4302. Respondents should be aware that notwithstanding any other provision of law, no person shall be subject to a penalty for failing to comply with a collection of information if it does not display a currently valid OMB control number.					
1. REPORT DATE 06 DEC 2007		2. REPORT TYPE Final		3. DATES COVERED 24-03-2006 to 23-09-2007	
4. TITLE AND SUBTITLE High-Temperature Ferromagnetism in Cr- and Mn-Implanted AlxGa1-xN				5a. CONTRACT NUMBER FA520906P0213	
				5b. GRANT NUMBER	
				5c. PROGRAM ELEMENT NUMBER	
6. AUTHOR(S) Mee-Yi Ryu				5d. PROJECT NUMBER	
				5e. TASK NUMBER	
				5f. WORK UNIT NUMBER	
7. PERFORMING ORGANIZATION NAME(S) AND ADDRESS(ES) Kangwon National University,192-1 Hyoja 2-Dong,Chuncheon, Kangwon-Do 200-701,Korea (South),KS,N/A				8. PERFORMING ORGANIZATION REPORT NUMBER N/A	
9. SPONSORING/MONITORING AGENCY NAME(S) AND ADDRESS(ES) AOARD, UNIT 45002, APO, AP, 96337-5002				10. SPONSOR/MONITOR'S ACRONYM(S) AOARD-064015	
				11. SPONSOR/MONITOR'S REPORT NUMBER(S)	
12. DISTRIBUTION/AVAILABILITY STATEMENT Approved for public release; distribution unlimited					
13. SUPPLEMENTARY NOTES					
14. ABSTRACT The work focused on optimization of ferromagnetism in the AlxGa1-xN materials system. That includes a systematic investigation of annealing temperature effects on magnetic, electrical, and optical properties of Cr-, Mn-, and Ni-implanted AlxGa1-xN, and optimization of the thermally stable, single phase, and room temperature ferromagnetic AlGaCrN, AlGaNiN, and/or AlGaMnN.					
15. SUBJECT TERMS					
16. SECURITY CLASSIFICATION OF:			17. LIMITATION OF ABSTRACT Same as Report (SAR)	18. NUMBER OF PAGES 21	19a. NAME OF RESPONSIBLE PERSON
a. REPORT unclassified	b. ABSTRACT unclassified	c. THIS PAGE unclassified			

I. Introduction

This is a final report of “High-temperature ferromagnetism in Cr- and Mn-implanted $\text{Al}_x\text{Ga}_{1-x}\text{N}$ ” for the period from 24 March 2006 – 23 September 2007 under AOARD Contract # FA5209-06-P-0213 at the Kangwon National University.

This research involves the collaboration with Prof. Yung Kee Yeo of Air Force Institute of Technology (AFIT), WPAFB, OH. Close collaboration with AFIT keeps the Kangwon National University program very much at fore front of the latest advancements that might influence spintronic device research.

II. Objectives

The purpose of this research is to investigate the magnetic properties of Cr- and Mn-implanted $\text{Al}_x\text{Ga}_{1-x}\text{N}$ along with their electrical and optical properties. The objective of the research is to determine optimal conditions for fabricating thin films of $\text{Al}_x\text{Ga}_{1-x}\text{N}$ that display ferromagnetism. Although recent advances in ion-implantation doping of group-III nitrides with Cr and Mn are making progress, efficient and controlled doping of $\text{Al}_x\text{Ga}_{1-x}\text{N}$ with Cr and Mn by the ion implantation technique remains a challenging problem. Therefore, we have performed a systematic investigation of annealing temperature effects on magnetic, electrical, and optical properties of Cr-, Mn-, and Ni-implanted $\text{Al}_x\text{Ga}_{1-x}\text{N}$ to produce a good, thermally stable, single phase, room temperature, ferromagnetic AlGaCrN , AlGaMnN , and/or AlGaNiN .

III. Research Results

In order to produce a dilute ferromagnetic wide-bandgap semiconductor at above room temperature, transition metal ions such as Cr, Ni, and Mn are implanted into host semiconductors of $\text{Al}_{0.35}\text{Ga}_{0.65}\text{N}$. 1- μm $\text{Al}_{0.35}\text{Ga}_{0.65}\text{N}$ was grown on an AlN buffer layer which was grown on a sapphire substrate by molecular beam epitaxial (MBE) method. Cr, Ni or Mn ions were implanted into $\text{Al}_{0.35}\text{Ga}_{0.65}\text{N}$ at an ion energy of 200 keV with a dose ranging from $5 \times 10^{16}/\text{cm}^2$ (average volume concentrations of 5 at.%) at room temperature by Implant Sciences in USA. After implantation, the samples were annealed from 675 to 775 °C at AFIT in an Oxy-Gon furnace using the rapid thermal annealing method in an N_2 environment for 5 min to anneal out the implantation damage.

The magnetic moment of each sample was measured using superconducting quantum interference device (SQUID) magnetometer. The SQUID measurements involved both variable-field measurements to determine the presence of magnetic hysteresis and temperature-dependent magnetization to determine the temperature range in which ferromagnetism persists as well as the presence of possible secondary magnetic phases. The temperature-dependent measurements have been made in both field-cooled (FC) and zero-field-cooled (ZFC) configurations. In FC measurements, the sample is cooled from room temperature to 5 K with a 500 Oe magnetic field applied to the sample, while in ZFC measurements, the sample is cooled to 5 K with no magnetic field applied before magnetic moment measurements begin.

A. Ferromagnetic properties of Nickel-implanted $\text{Al}_{0.35}\text{Ga}_{0.65}\text{N}$ (Accepted for publication in the Journal of the Korean Physical Society)

1. Introduction

The possibility for room-temperature applications of spin-transport electronic (spintronic) devices has led to an increased interest in doping wide-bandgap semiconductors with transition metals [1-5]. Much of this interest has been focused on GaN, but the ternary AlGaIn possesses similar desirable properties for spin-based applications such as spin transistors and polarized light emitters [6-8]. The most prominent methods for doping wide-bandgap semiconductors for spintronic purposes are ion implantation and doping during epitaxial growth. The advantages of ion implantation technique include superior control of dopant dose, control of implantation areas to allow for device formation, and separating growth and doping processes. Separation of crystal growth and doping is important in the case of wide-bandgap semiconductor materials doped with transition metals, particularly when simultaneously doping the material with donors or acceptors, because successful incorporation of transition metals requires somewhat extraordinary growth conditions [9-13].

Accordingly, the research reported here concerns the optical and magnetic properties of Ni-implanted $\text{Al}_{0.35}\text{Ga}_{0.65}\text{N}$ with the focus being on finding optimal annealing conditions for the realization of a dilute magnetic semiconductor (DMS). We report the fabrication of a DMS material in which magnetic properties persist to a temperature of at least 350 K (77 °C) by implanting $\text{Al}_{0.35}\text{Ga}_{0.65}\text{N}$ with Ni and annealing at or above 700 °C for 5 min.

2. Experiment

The undoped $\text{Al}_{0.35}\text{Ga}_{0.65}\text{N}$ film was grown by molecular beam epitaxy (MBE) atop an AlN buffer layer on a sapphire substrate. The $\text{Al}_{0.35}\text{Ga}_{0.65}\text{N}$ film thickness was about 1 μm and

an amorphous cap layer of 500 Å thick AlN was deposited as the uppermost layer of the film. Both ion implantation and subsequent annealing took place with this capping layer in place, but it was removed using a solution of 0.5 M KOH before optical or magnetic measurements. The ion implantation was performed at room temperature with an implant energy of 200 keV to a dose of $3 \times 10^{16} \text{ cm}^{-2}$. These implantation parameters correspond to a peak concentration of $3.45 \times 10^{21} \text{ cm}^{-3}$ at a projected range of 1009 Å under the surface (509 Å below the surface of the $\text{Al}_{0.35}\text{Ga}_{0.65}\text{N}$ film after removing the AlN cap layer). After implantation, the samples were annealed in an Oxy-Gon annealing furnace at temperatures between 650 and 775 °C for 5 min. Before annealing, each $\text{Al}_{0.35}\text{Ga}_{0.65}\text{N}$ sample was wrapped face-to-face with a GaN sample that was also implanted with Ni ions. The proximity cap annealing was conducted in an atmosphere of pure nitrogen flowing at 2 L/min.

The optical properties of the samples were characterized by cathodoluminescence (CL) to determine the effects of ion implantation and damage recovery after subsequent annealing. The CL measurements were made at an electron beam energy of 10 keV and a beam current of 50 μA. Direct magnetic moment measurements, as a function of applied magnetic field and temperature, were made using a superconducting quantum interference device (SQUID).

3. Results and discussion

Cathodoluminescence was measured at 5 K for Ni-implanted $\text{Al}_{0.35}\text{Ga}_{0.65}\text{N}$ annealed at various temperatures in flowing nitrogen gas for 5 min, and the results are shown in Fig. 1 along with spectra for as-grown and as-implanted $\text{Al}_{0.35}\text{Ga}_{0.65}\text{N}$ samples. As shown in the figure, the as-grown sample is characterized by strong luminescence in the ultraviolet (UV) region of the spectrum centered at 4.4 eV and a much smaller broader blue-green peak centered at 2.5 eV. The luminescence peak at 4.4 eV is attributed to band-edge transitions, involving unresolved, combined peaks from donor-bound excitons, donor-acceptor pairs, and their phonon replicas [14]. The as-implanted sample shows practically no luminescence at all.

As evidenced in Fig. 1, the band-edge luminescence peak was not observed for all the implanted and annealed samples. However, the annealing leads to the emergence of a strong, broad CL peak in the green region of the spectrum centered at 2.35 eV as well as much less intense peaks centered in the violet band at 3.1 eV and UV band at 3.8 eV. The jagged appearance of the 2.35 eV peaks is due to Fabry-Perot type interference. The intensities of both the green and violet luminescence bands increase as anneal temperature increases. Similar CL features were reported for Si-implanted $\text{Al}_{0.25}\text{Ga}_{0.75}\text{N}$ [15], exhibiting very broad yellow and green bands at slightly different energies of 2.26 and 2.32 eV, respectively. However, these yellow and green bands appear only after annealing at 1000 °C or higher, whereas these bands appear even after 650 °C anneal. They observed that both the green band

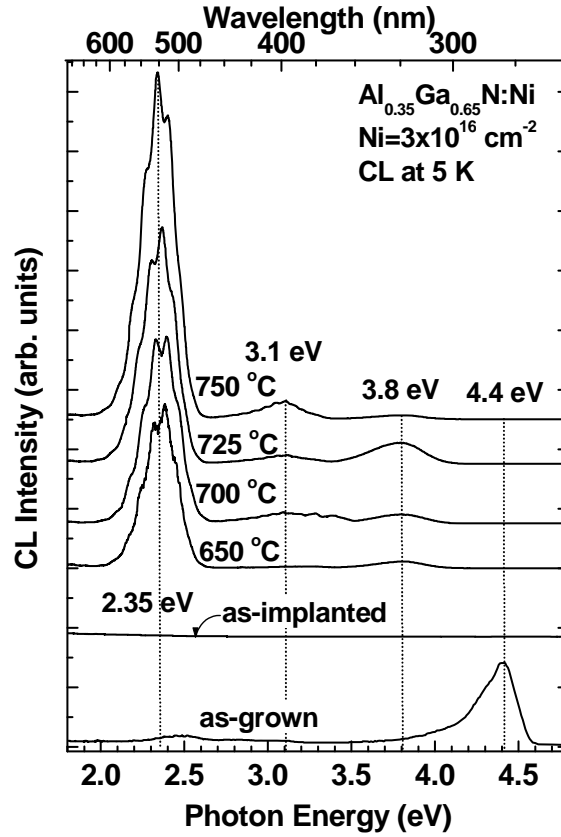


Fig. 1. CL spectra taken at 5 K for $\text{Al}_{0.35}\text{Ga}_{0.65}\text{N}$ implanted with Ni ions at 200 keV to a dose of $3 \times 10^{16} \text{ cm}^{-2}$ and annealed at various temperatures for 5 min.

and Si activation increases with annealing temperature, and thus, the green band is related to Si-donor activation. We believe that a similar phenomenon is occurring in Ni-implanted $\text{Al}_{0.35}\text{Ga}_{0.65}\text{N}$, and thus the 2.36 eV (green) and 3.10 eV (violet) peaks, which are not present in the as-grown sample and only manifest themselves after annealing, are believed to be related to the activation of implanted Ni impurities and/or implantation-damage related defects. The broad peak centered around 3.82 eV is attributed to Al-N-O complexes at the substrate-AlN buffer layer interface [16]. Although the implanted and annealed samples do not show bandedge luminescence due to the large amount of Ni impurities, they certainly indicate that significant implantation related damage has been recovered. All these CL observations agree well with the results of magnetic moment measurements discussed below, which show that coercivity increases with annealing temperature up to 750 °C.

The magnetic properties of Ni-implanted $\text{Al}_{0.35}\text{Ga}_{0.65}\text{N}$ have been investigated as a function of annealing temperature from 650-775 °C using a SQUID magnetometer. The results of magnetic moment measurements taken at 5 and 300 K are plotted in Fig. 2 as a

function of magnetic field along with the as-grown and as-implanted (not annealed) samples. For clarity only data taken at 5 and 300 K are shown in the figure, although measurements have been taken at additional temperatures.

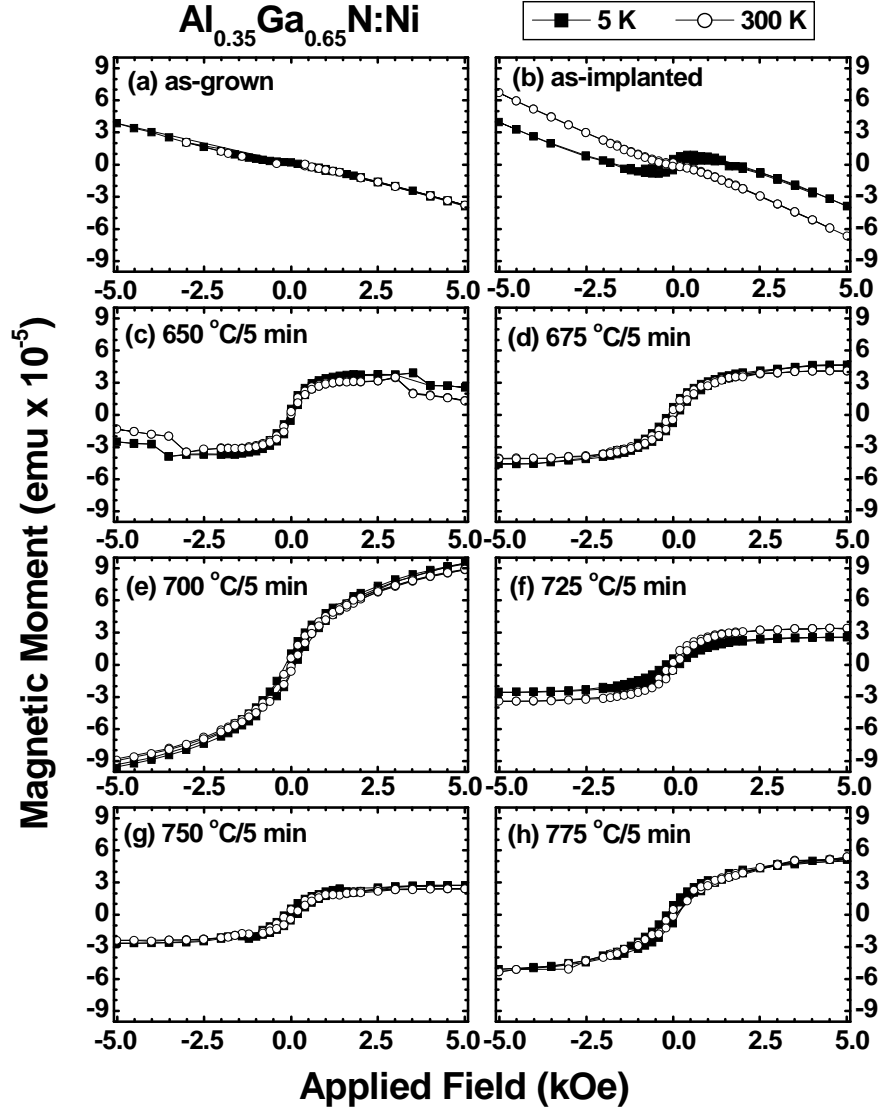


Fig. 2. Variable field magnetization measurements taken at 5 and 300 K for Ni-implanted $\text{Al}_{0.35}\text{Ga}_{0.65}\text{N}$ annealed from 650 to 775 °C for 5 min. Raw data (diamagnetic background not subtracted) are also presented for the as-grown and as-implanted samples.

The as-grown sample (Fig. 2a) clearly shows linear diamagnetic behavior at both room temperature and 5 K that is mainly attributable to the sapphire substrate. The as-implanted sample (Fig. 2b) also shows predominately diamagnetic behavior at room temperature, but at 5 K it shows a ferromagnetic hysteresis loop superimposed on the diamagnetic component. It is believed that this ferromagnetic appearance is due to the behavior of monatomic Ni interstitials in the $\text{Al}_{0.35}\text{Ga}_{0.65}\text{N}$ lattice [17]. As such these magnetic properties are not useful for the fabrication of DMS-based electronics. Upon annealing, all the samples show hysteresis loops indicative of ferromagnetic behavior in variable field measurements, but the diamagnetic background effect remains present in the measured data for all samples regardless of annealing conditions, and thus affects the magnetization curves taken at 5 and 300 K.

Since the diamagnetic component due mainly to the sapphire substrate significantly affects the magnetization curve, it was corrected in order to obtain the true magnetic properties of the annealed samples owing to the Ni implantation, and the corrected results are shown in Fig. 2(c-h). To perform this correction, the linear diamagnetic component as a function of magnetic field has been removed for each data point. The specific correction used here is that the background diamagnetism is removed by rotating each data point comprising the variable field measurement about the origin by an identical angle. The angle is determined by what is necessary to cause the linear region observed above saturation to be parallel to the x -axis.

Variable field measurements reveal that the sample annealed at 700 °C for 5 min demonstrates the greatest dominance of ferromagnetism as well as the highest saturation magnetization. For this sample, a higher applied field of approximately 8 kOe was required to induce magnetic saturation. These measurements also show that the magnetic signatures of ferromagnetism (hysteretic separation and saturation) persist to room temperature in the samples annealed between 675 and 775 °C. The sample annealed at 650 °C for 5 min is superparamagnetic since it shows clear magnetic saturation but negligible hysteretic separation.

The coercive and remanent fields for the measurements shown in Fig. 2 are detailed in table 1. These data have linear diamagnetic influences removed before determination of the coercive and remanent fields. As shown in table 1 and Fig. 2, the coercive field increases up to 222 Oe at 5 K and 118 Oe at room temperature as the anneal temperature increases up to 750 °C and then it decreases. According to the strength of the coercive field, the sample annealed at 750 °C for 5 min shows the strongest ferromagnetic behavior. This sample also displays the greatest remanent fields (as a percentage of saturation magnetization) at both 5 K (22%) and room temperature (16%) with similar values for the sample annealed at 725 °C.

The sample annealed at 700 °C shows promise because it has the highest saturation magnetic moment as seen in the magnetization data in Fig. 2.

Table 1. Coercive (H_c) and remanent fields (B_R) at 5 and 300 K for various annealing conditions in Ni-implanted $\text{Al}_{0.35}\text{Ga}_{0.65}\text{N}$. Coercive fields given are an average of the positive- and negative-going zero magnetization crossings. Remanent fields are reported as a percentage of saturation magnetization (M_S), which also varies with annealing temperature.

Annealing Conditions		Coercive Fields (O_e)		Remanent Fields (% of M_S)	
Temp (°C)	Time (min)	5 K	300 K	5 K	300 K
650	5	75	41	16	8
675	5	136	88	16	13
700	5	167	98	17	12
725	5	191	95	23	14
750	5	222	118	22	16
775	5	165	94	17	7

For the sample annealed at 700 °C for 5 min, hysteresis measurements were also made as a function of sample temperature at seven temperatures from 5 to 350 K. For clarity, only three representative results of these measurements are depicted in Fig. 3. These measurements have the as-grown (unimplanted) background subtracted (with weight discrepancies factored). The coercive field decreases from 167 to 98 Oe and the remanent field decreases from 16.5 to

12.2% of M_S value of $\sim 10^{-4}$ emu as the sample temperature increases from 5 to 350 K. The data collected at temperatures between those reported followed the trend of decreasing coercive and remanent field strengths with increasing sample temperature.

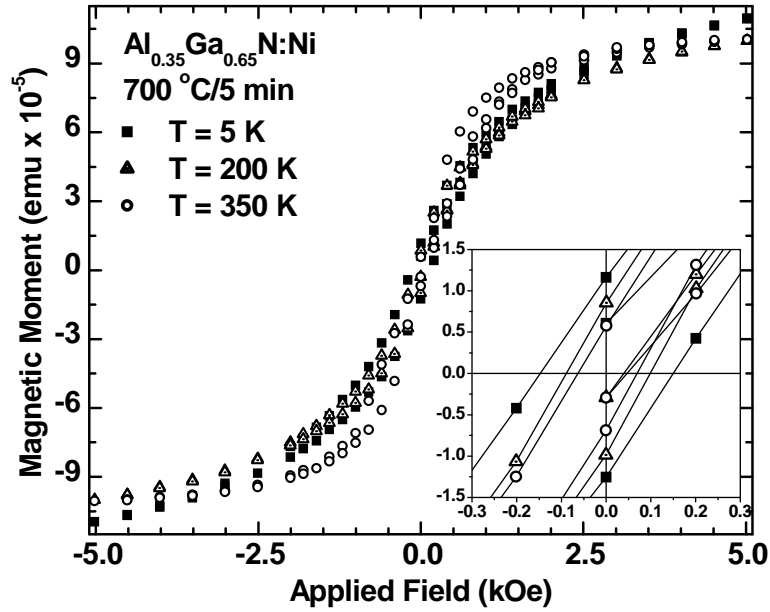


Fig. 3. Variable field measurements taken at temperatures of 5, 200, and 350 K for Ni-implanted Al_{0.35}Ga_{0.65}N annealed at 700 °C for 5 min. The inset is a close-up view of magnetic behavior near the origin to show the effect of temperature on remanent and coercive field strengths.

Figure 4 shows the magnetic measurements of Ni-implanted Al_{0.35}Ga_{0.65}N annealed at various temperatures as a function of sample temperature under both field-cooled (FC) and zero-field-cooled (ZFC) conditions. A probing field of 500 Oe was used during both measurements and during field cooling. For the as-grown sample, the FC and ZFC magnetization curves have no separation at all until the sample temperature falls below 50 K, where the FC magnetization begins to increase rapidly. The as-implanted sample shows almost no separation between FC and ZFC magnetization curves as seen in the figure. The divergence between FC and ZFC magnetization below 50 K in the as-implanted sample is explained by the presence of a spin-glass phase. When cooled without an applied field, the material “freezes” into a state of frustrated magnetic ordering with a smaller magnetic moment arising from the Ni-implanted Al_{0.35}Ga_{0.65}N, so that the sample is more dominated by

the background diamagnetism. As the sample is warmed, the frustrated magnetic ordering is lost due to thermal effects, so the net magnetic moment rises. When the material is cooled in the presence of the 500 Oe probing field, the magnetic ordering is not frustrated and so the total magnetic moment rises as thermal disordering effects are reduced.

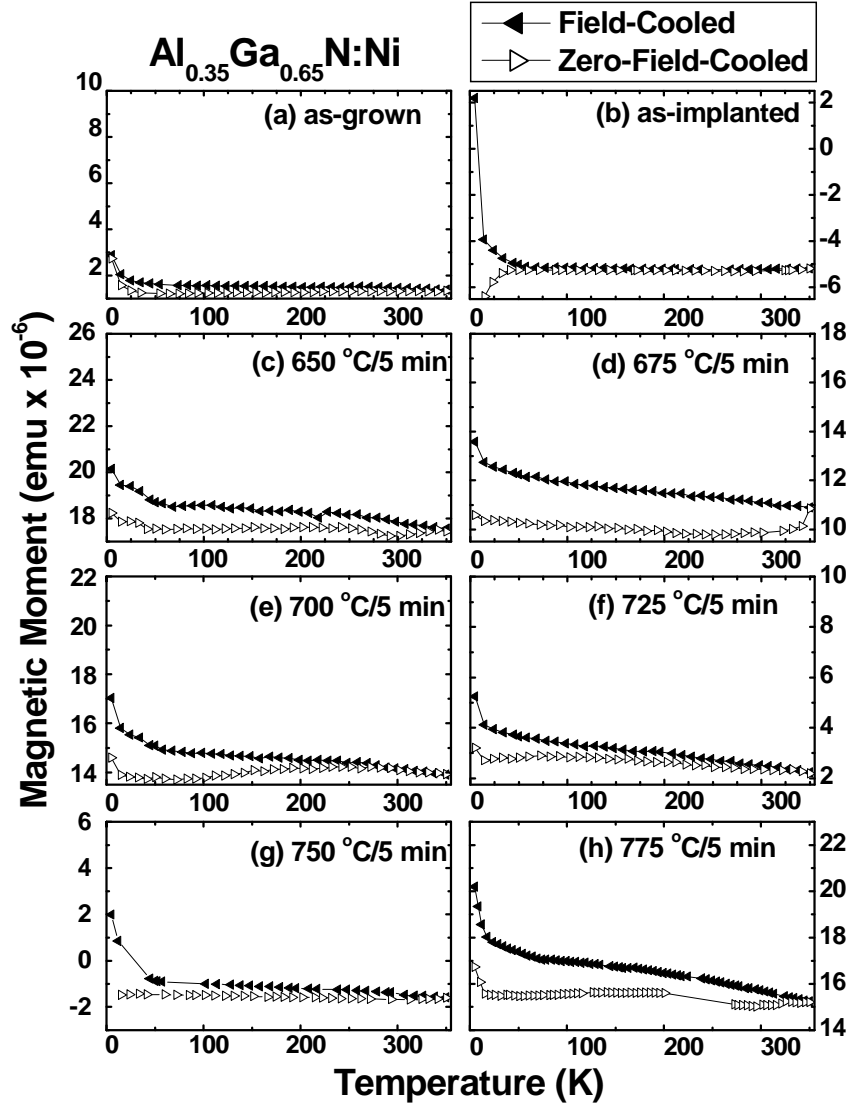


Fig. 4. Variable temperature measurements on $\text{Al}_{0.35}\text{Ga}_{0.65}\text{N}$ samples implanted with Ni and annealed at various temperatures for 5 min.

By contrast, all of the annealed samples show hysteretic behavior persisting to room temperature (Fig. 2(c-h)) as well as clear FC-ZFC magnetization separation in temperature-

dependent measurements. The data presented in Figs. 2 and 4 show that ferromagnetism is present in annealed $\text{Al}_{0.35}\text{Ga}_{0.65}\text{N}:\text{Ni}$ at temperatures up to (and probably above) 350 K (77 °C). The difference between annealed and unannealed samples is clarified by the fact that the as-implanted sample shows a predominantly diamagnetic character at room temperature and has almost no separation between FC and ZFC magnetization curves as seen in Fig. 4. Further indication that this material is dominated by a ferromagnetic phase is seen in Fig. 4 where FC and ZFC magnetization measurements are separated and track together at low temperatures, which occurs due to the decrease in random thermal effects that tend to reduce magnetic ordering. Testing at temperatures above 350 K was not possible due to limitations of the equipment used, so the lack of difference between FC and ZFC magnetization at 350 K may be due to equipment limitations more than physical phenomenon occurring in the dilute magnetic semiconductor. The presence of a “hump” in the ZFC data in the samples annealed at and above 700 °C indicates that there may be a spin-glass phase present concurrently with the dominant ferromagnetic phase. Minimizing the presence of this phase will allow for more efficient use of the implanted Ni from a magnetic ordering standpoint.

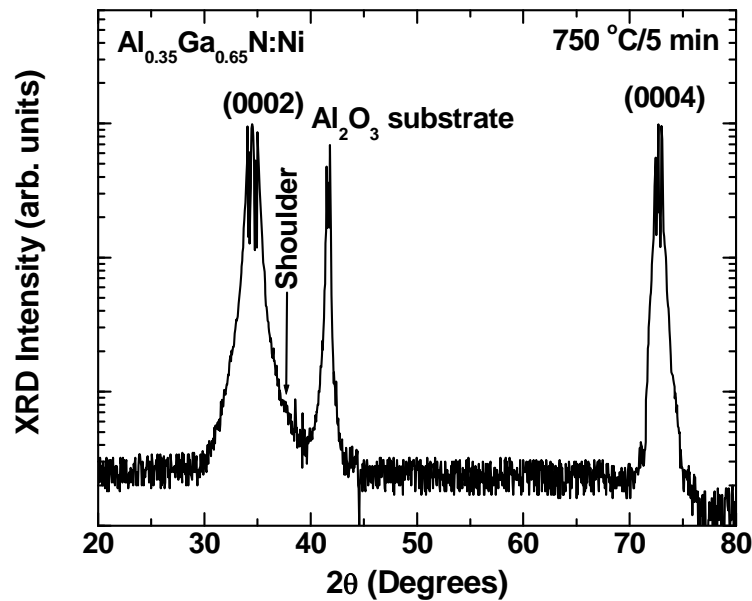


Fig. 5. X-ray diffraction data from Ni-implanted $\text{Al}_{0.35}\text{Ga}_{0.65}\text{N}$ annealed at 750 °C for 5 min.

In order to verify implantation damage recovery and to rule out secondary phases as the source of ferromagnetism in the Ni-implanted $\text{Al}_{0.35}\text{Ga}_{0.65}\text{N}$ sample annealed at 750 °C for 5 min, X-ray diffraction (XRD) measurements were also performed using $\text{Cu-K}\alpha$ radiation

($\lambda=1.5418 \text{ \AA}$). The results of the 2θ scan are shown in Fig. 5. The line seen around 34.5° in the 2θ scan is a result of reflections from the (0002) plane of AlGa_{0.35}N [18,19]. The weak shoulder to the right of peak at 34.5° indicates the presence of DMS material [20]. Its low intensity, compared to the (0002) peak, is explained by the fact that only a fraction of the volume of the Al_{0.35}Ga_{0.65}N contains the implanted Ni. The peak at around 74° occurs because of reflections from the (0004) plane in AlGa_{0.35}N [18]. The peak at 43.3° indicates reflection from the (113) plane of the Al₂O₃ substrate [21].

The consistency of XRD data between as-grown AlGa_{0.35}N films reported in literatures [18, 19] and the Al_{0.35}Ga_{0.65}N implanted with Ni and annealed at 750°C for 5 min indicates that the implant damage has been largely recovered by the annealing performed on this sample. Possible secondary ferromagnetic phases (Ni²², Ni₃Al²³, and Ni₃Ga, assuming similarity to Ni₃Al) have been eliminated as sources for the shoulder to the right of the (0002) AlGa_{0.35}N peak by XRD measurements reported for Ni and Ni₃Al [22,23].

4. Conclusions

Magnetic characterization studies have been conducted using SQUID magnetometry on MBE-grown Al_{0.35}Ga_{0.65}N implanted with Ni at room temperature with an energy of 200 keV to a dose of $3 \times 10^{16} \text{ cm}^{-2}$ and annealed at various temperatures in flowing nitrogen gas. It has been found that the ferromagnetic properties and implantation damage recovery are dependent upon anneal temperature, but all the materials show clear signs of ferromagnetism after annealing between 675 and 775°C for 5 min. The ferromagnetic property persists above room temperature, and at an optimum anneal temperature of around 750°C , a coercive field width of 118 Oe and a remanent field of 16% of the saturation magnetization of $2.6 \times 10^{-5} \text{ emu}$ were obtained at 300 K. Field-cooled (FC) and zero-field-cooled (ZFC) magnetization measurements as a function of sample temperature also indicate the presence of a ferromagnetic phase in this material, although there may be a weak spin-glass phase competing with the ferromagnetism. The Curie temperature is estimated to be around 350 K. Although bandedge luminescence is absent from the implanted and annealed samples, the variation of CL intensity as a function of anneal temperature indicates that significant implantation-related damage has been recovered after annealing. The XRD measurements also confirm that the lattice structure of Ni-implanted sample is recovered well after annealing at 750°C for 5 min, indicating good Ni incorporation into the Al_{0.35}Ga_{0.65}N. Furthermore, XRD measurements also show no indication of secondary phase formation and/or clusters involving Ni. Thus, the observed ferromagnetism in this material can be attributed to Ni incorporation into Al_{0.35}Ga_{0.65}N, forming a dilute ferromagnetic semiconductor.

ACKNOWLEDGEMENTS

The authors would like to thank Dr. D. Silversmith and Dr. T. Steiner of the Air Force Office of Scientific Research for supporting this work and Virginia Commonwealth University for the use of their SQUID system during initial magnetic characterization of selected samples. Mee-Yi Ryu would like to thank Dr. M. Mah of the Asian Office of Aerospace Research and Development for supporting this work.

REFERENCES

- [1] T. Jungwirth, J. Sinova, J. Kučera, A.H. MacDonald, *Current Appl. Phys.* **3**, 461 (2003).
- [2] T. Dietl, H. Ohno, F. Matsukura, J. Cibert, D. Ferrand, *Science* **287**, 1019 (2000).
- [3] Y. Uspenskii, E. Kulatov, H. Mariette, H. Nakayama, H. Ohta, *J. Magnetism and Magnetic Mat.* **258-259**, 248 (2003).
- [4] T. Dietl, *Semicon. Science and Tech.* **17**, 377 (2002).
- [5] C.Y. Fong, V.A. Gubanov, C. Boekema, *J. Elect. Mat.* **29**, 1067 (2000).
- [6] R.M. Frazier, G.T. Thaler, C.R. Abernathy, S.J. Pearton, M.L. Nakarmi, K.B. Nam, J.Y. Lin, H.X. Jiang, J. Kelly, R. Rairigh, A.F. Hebard, J.M. Zavada, R.G. Wilson *J. Appl. Phys.* **94**, 4956 (2003).
- [7] S.J. Pearton, C.R. Abernathy, M.E. Overberg, G.T. Thaler, D.P. Norton, N. Theodoropoulou, A.F. Hebard, Y.D. Park, F. Ren, J. Kim, L.A. Boatner, *J. Appl. Phys.* **93**, 1 (2003).
- [8] S. Das Sarma, J. Fabian, X. Hu, and I. Žutić, *Proc. 58th Device Research Conf., IEEE, Denver, USA, 2000*, p95.
- [9] S. Sonoda, H. Hori, Y. Yamamoto, T. Sasaki, M. Sato, S. Shimizu, K. Suga, K. Kindo, *IEEE Transactions on Magnetics* **38**, 2859 (2002).
- [10] R. Dwiliński, R. Doradziński, J. Garczyński, L. Sierzputowski, J.M. Baranowski, M. Kamińska, *Diamond and Related Mat.* **7**, 1348 (1998).
- [11] H. Akinaga, S. Németh, J. De Boeck, L. Nistor, H. Bender, G. Borghs, H. Ofuchi, M. Oshima, *Appl. Phys. Lett.* **77**, 4377 (2000).
- [12] S. Sonoda, S. Shimizu, T. Sasaki, Y. Yamamoto, H. Hori, *Condensed Matter* **0108**, 159 (2001).
- [13] S. Kuwabara, T. Kondo, T. Chikyow, P. Ahmet, H. Munekata, *Japan. J. Appl. Phys. Part 2* **40**, L724 (2001).
- [14] J.L. McFall, R.L. Hengehold, Y.K. Yeo, J.E. Van Nostrand, A.W. Saxler, *J. Crys. Growth* **227-228**, 458 (2001).

- [15] M.-Y. Ryu, E.A. Chitwood, E.N. Claunch, Y.K. Yeo, R.L. Hengehold, J.A. Fellows, T. Steiner, *Phys. Sta. Sol. (c)* **0**, 2593 (2003).
- [16] X.L. Sun, S.H. Goss, L.J. Brillson, D.C. Look, R.J. Molnar, *J. Appl. Phys.* **91**, 6729 (2002).
- [17] P.W. Selwood, *Adsorption and Collective Paramagnetism*, chapter 3, pages 35-50, Academic Press, London, 1962.
- [18] D. Korakakis, K.F. Ludwig, Jr., T.D. Moustakas, *Appl. Phys. Lett.* **71**, 72 (1997).
- [19] T.D. Moustakas, *Gallium-Nitride-based Technologies*, chapter 1, Critical Reviews, SPIE Optical Engineering Press, Bellingham, Washington, 2002, pp 1-46.
- [20] J.S. Lee, J.D. Lim, Z.G. Khim, Y.D. Park, S.J. Pearton, S.N.G. Chu, *J. Appl. Phys.* **93**, 4512 (2003).
- [21] A. Golubović, S. Nikolić, S. Djurić, A. Valčić, *J. Serbian Chem. Soc.* **66**, 411 (2001).
- [22] A. Antolak, M. Krasnowski, T. Kulik, *Rev. on Advanced Mat. Sci.* **8**, 111 (2004).
- [23] J.Y. Rhee, Y.V. Kudryavtsev, Y.P. Lee, *Phys. Rev. B* **68**, 045104 (2003).

B. Room temperature ferromagnetic properties of transition metal implanted $\text{Al}_{0.35}\text{Ga}_{0.65}\text{N}$ (Published in the Journal of Alloys and Compounds 423 (2006), 184-187)

1. Introduction

The potential for room temperature ferromagnetism in a semiconductor material has led to much work involving doping wide-bandgap semiconductors with transition metals (TMs) [1–5]. AlGa_{0.65}N is among the materials that will be useful for spin transport electronics (spintronics) applications such as spin transistors or polarized light emitters when doped with TMs [6–8]. Doping with transition metals during epitaxial growth of wide-bandgap semiconductors requires unusual growth conditions [9–13], which can lower the quality of the semiconductor material as well as cause problems with the incorporation of n- or p-type dopants. Ion implantation of TMs avoids these difficulties associated with incorporating them during the growth process as well as allowing for more precise dosage and lateral control of the dopant profile. The implantation process, however, does induce damage in the semiconductor crystal, and thus proper annealing must be performed to remove this damage.

2. Experiment

A nominally undoped Al_{0.35}Ga_{0.65}N was implanted with Cr, Mn, or Ni at room temperature with an ion energy of 200 keV and annealed at temperatures between 650 and 800 °C in an

atmosphere of flowing nitrogen gas. Evidence of the implantation damage recovery was evaluated using cathodoluminescence (CL) measurements. Based on the Hall effect measurements performed on similar AlGa_{0.35}N samples, the nominally undoped Al_{0.35}Ga_{0.65}N is an n-type with a room-temperature free carrier concentration on the order of 10^{12} cm^{-3} . The magnetic moment of each sample was measured using superconducting quantum interference device (SQUID) magnetometer. The SQUID measurements involved both variable-field measurements to determine the presence of magnetic hysteresis and temperature dependent magnetization to determine the temperature range in which ferromagnetism persists as well as the presence of possible secondary magnetic phases. The temperature-dependent measurements have been made in both field-cooled (FC) and zero-field-cooled (ZFC) configurations. In FC measurements, the sample is cooled from room temperature to 5 K with a 500 Oe magnetic field applied to the sample, while in ZFC measurements, the sample is cooled to 5 K with no magnetic field applied before magnetic moment measurements begin.

3. Results and discussion

3.1. Cr-implanted Al_{0.35}Ga_{0.65}N

The results of variable magnetic field measurements performed at both 5 and 300 K are shown in Fig. 1(a) for the Cr-implanted Al_{0.35}Ga_{0.65}N with a dose of $5 \times 10^{16} \text{ cm}^{-2}$ and annealed at a temperature of 750 °C for 5 min in a flowing nitrogen atmosphere. The data shown here are corrected for the diamagnetic background of the sapphire substrate. For this sample, the hysteresis curve shows a coercive field (H_C) width of 308 Oe at 5 K and 178 Oe at 300 K. The data presented in Fig. 1(a) also indicate saturation magnetization (M_S) values of 0.35 Bohr magneton (μ_B) per implanted Cr atom at both 5 and 300 K. The maximum atomic magnetic moment value calculated for Cr^{2+} ion is $4.8 \mu_B$ [14, Table 31.4]. The remanent field (B_R) values are 17% and 11%, respectively, as a fraction of M_S values of $3 \times 10^{-5} \text{ emu}$ at both 5 and 300 K. Temperature-dependent magnetization measurements on the Cr-doped Al_{0.35}Ga_{0.65}N sample annealed at 750 °C also indicate ferromagnetism. As depicted in Fig. 1(b), the separation between field-cooled (FC) and zero-field-cooled (ZFC) magnetization values is evident and both magnetization curves move steadily together as temperature decreases.

The CL measurements, which are not shown here, have an increasingly intense blue-green peak as annealing temperature is raised from 650 to 750 °C. Because of similar behavior in Si-implanted Al_{0.25}Ga_{0.75}N [16], this observation is believed to stem from increasing incorporation of the Cr into the Al_{0.35}Ga_{0.65}N crystal lattice.

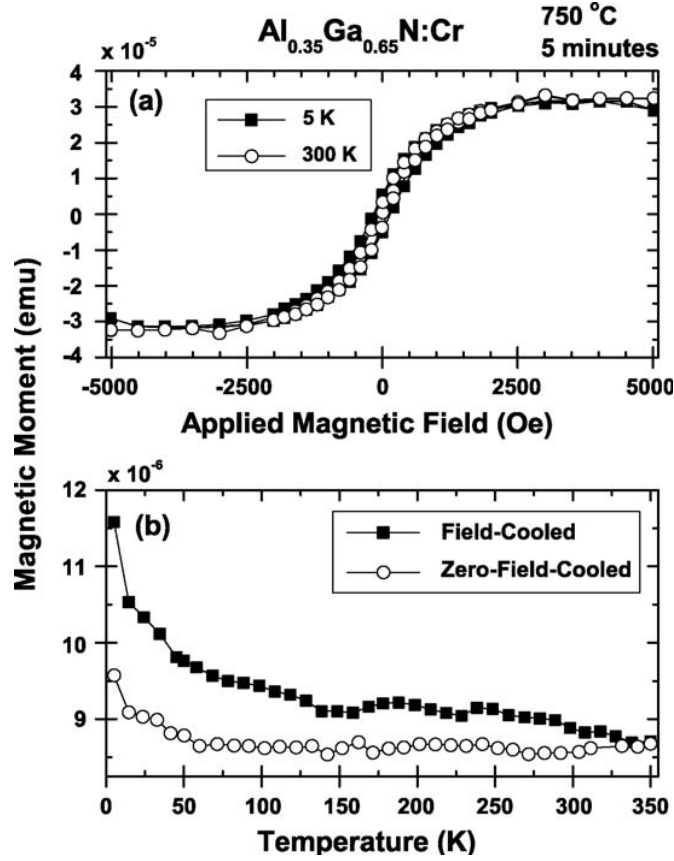


Fig. 1. (a) Hysteresis loops of variable magnetic field measurements performed at 5 and 300 K on $\text{Al}_{0.35}\text{Ga}_{0.65}\text{N}$ implanted with Cr and annealed at 750°C for 5 min in flowing nitrogen gas. The diamagnetic contribution of the sapphire substrate has been removed in the data presented. (b) Temperature-dependent magnetization measurements, under both zero-field-cooled and field-cooled (at 500 Oe) conditions, for Cr-implanted $\text{Al}_{0.35}\text{Ga}_{0.65}\text{N}$ annealed for 5 min at 750°C in flowing N_2 .

Because of the strong indications of ferromagnetism by hysteresis curve and FC–ZFC curve separation, and the CL measurements showing reasonable damage recovery, Cr-implanted $\text{Al}_{0.35}\text{Ga}_{0.65}\text{N}$ is believed to be a true dilute ferromagnetic semiconductor (DMS) material. However, the possibility of these magnetic observations arising from clusters cannot be ruled out without experiments that confirm the interaction of the d-shell electrons from the transition metal with the conduction and/or valence bands of the semiconductor.

3.2. Mn-implanted $\text{Al}_{0.35}\text{Ga}_{0.65}\text{N}$

The corrected ferromagnetic hysteresis curve is shown in Fig. 2(a) for the $\text{Al}_{0.35}\text{Ga}_{0.65}\text{N}$

wafer implanted with Mn to a dose of $5 \times 10^{16} \text{ cm}^{-2}$ and annealed at 750 °C for 5 min in flowing N₂ gas. The value of H_C measured for this sample at 5 K is 279 Oe, and the H_C value measured at 300 K is 180 Oe. The value of M_S for the sample annealed at 750 °C is 0.34 μ_B per Mn atom at 5 K and 0.37 μ_B per Mn atom at 300 K. The maximum calculated magnetic moment per Mn²⁺ atom is 5.9 μ_B [14, Table 31.4]. The values of B_R , as a percentage of M_S , are 19% at 5 K and 11% at 300 K.

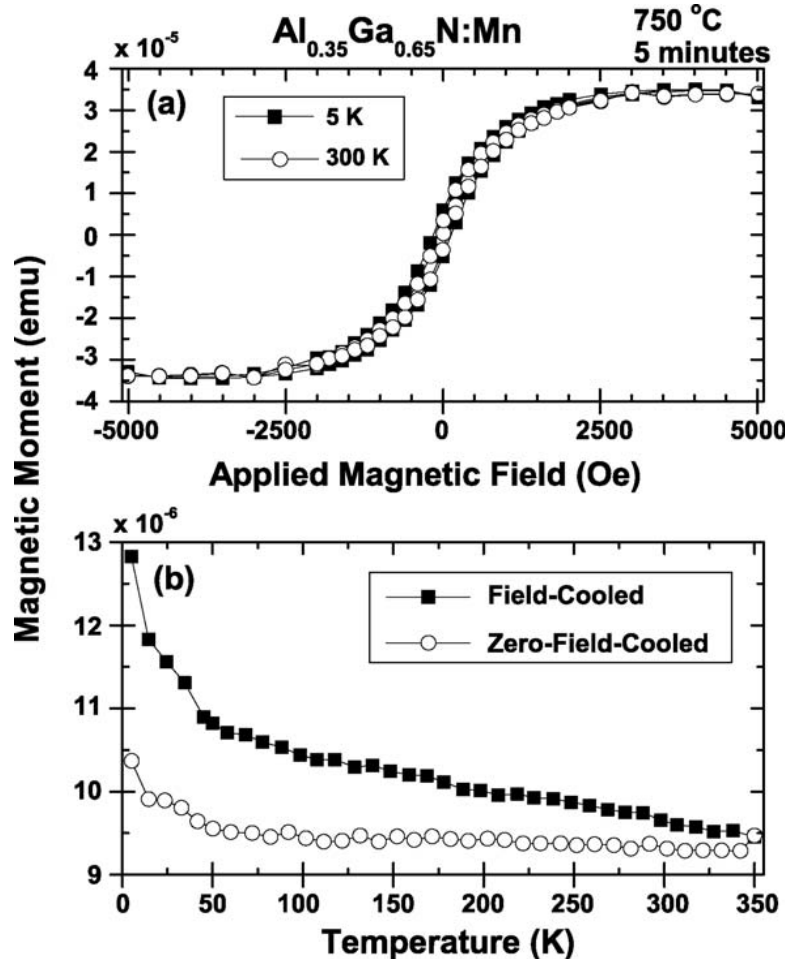


Fig. 2. (a) Hysteresis in variable magnetic field measurements performed at 5 and 300 K on Mn-implanted Al_{0.35}Ga_{0.65}N annealed at 750 °C for 5 min in flowing N₂ gas. Diamagnetic response from the sapphire substrate has been removed. (b) Results of magnetization vs. temperature measurements performed on Mn-implanted Al_{0.35}Ga_{0.65}N annealed at 750 °C for 5 min in flowing N₂ gas under zero-field-cooled and field-cooled (at 500 Oe) conditions.

Temperature-dependent magnetization measurements taken from $\text{Al}_{0.35}\text{Ga}_{0.65}\text{N}$ annealed at 750 °C for 5 min under both FC and ZFC conditions are shown in Fig. 2(b). The separation between FC and ZFC magnetization curves indicate the presence of ferromagnetism in this material. The FC–ZFC separation is greater overall in the sample annealed at 775 °C (not shown), but there is a slight rise in the ZFC values around 175 K that may be indicative of a spin-glass phase in this material when annealed at higher temperatures. Therefore, it should be further studied as a possible candidate material for spintronic devices. Because of the larger calculated magneton value from Mn^{2+} , the Mn-implanted $\text{Al}_{0.35}\text{Ga}_{0.65}\text{N}$ will allow for stronger magnetic moments even when maximum magnetic activation efficiency is not achieved.

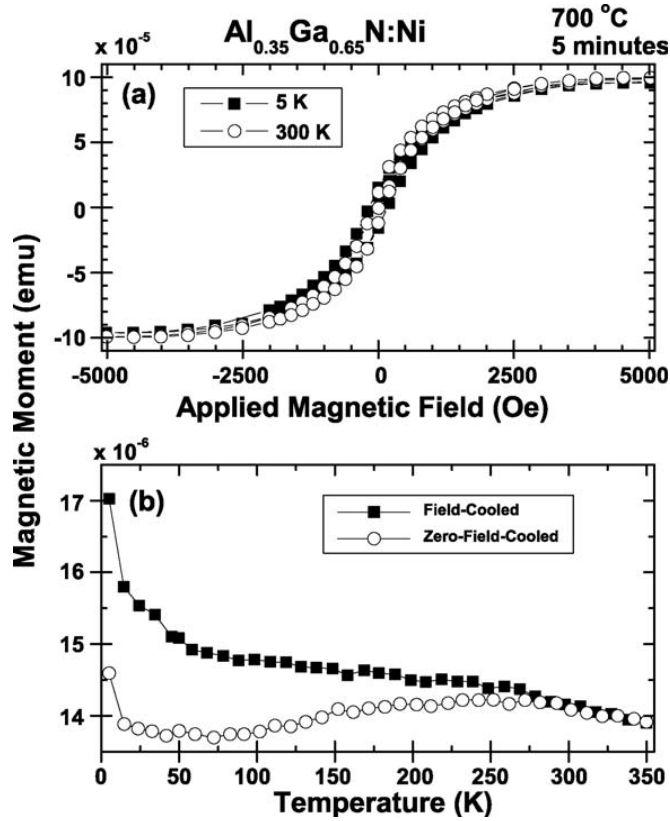


Fig. 3. (a) Magnetic hysteresis measurements at both 5 and 300 K for Ni implanted $\text{Al}_{0.35}\text{Ga}_{0.65}\text{N}$ annealed at 700 °C for 5 min in flowing nitrogen gas. Note that applied field scale is larger due to higher saturation magnetization in this sample. Although the contribution from the sapphire substrate is small compared to the saturation moment from this sample, the background diamagnetism has been removed. (b) Temperature-dependent magnetization measurements of Ni-implanted $\text{Al}_{0.35}\text{Ga}_{0.65}\text{N}$ annealed at 700 °C for 5 min in flowing N_2 under both field-cooled (at 500 Oe) and zero-field-cooled conditions.

3.3. Ni-implanted $\text{Al}_{0.35}\text{Ga}_{0.65}\text{N}$

The corrected hysteresis loops for the Ni-implanted $\text{Al}_{0.35}\text{Ga}_{0.65}\text{N}$ sample measured at 5 and 300 K are shown in Fig. 3(a). The strongest evidence of ferromagnetism occurs in the sample annealed at 700 °C for 5 min, showing H_C values of 334 and 195 Oe at 5 and 300 K, respectively. The M_S values determined from the hysteresis loops at both 5 and 300 K are $1.8 \mu_B$ per implanted Ni atom. The calculated magneton value for the Ni^{2+} ion is $3.2 \mu_B$ [14, Table 31.4]. This high value of M_S required an applied magnetic field of 10,000 Oe to induce magnetic saturation, which is the reason why the width of H_C in Fig. 3(a) appears smaller than in Figs. 1(a) and 2(a). The remanent fields are 17% and 12% of M_S at 5 and 300 K, respectively. Similar percentages are found in this material annealed at other temperatures.

The results of temperature-dependent magnetization measurements of Ni-implanted $\text{Al}_{0.35}\text{Ga}_{0.65}\text{N}$ annealed at 700 °C are shown in Fig. 3(b). Despite the strong evidence of ferromagnetism in variable field measurements, the magnetization versus temperature measurements of this sample show a lack of FC–ZFC separation at temperatures above 275 K. This is most likely due to the fact that hysteresis measurements tend to be more sensitive indicators of ferromagnetism at high temperatures than do FC–ZFC differences [15]. However, the fact that FC and ZFC magnetization curves track together at low temperatures with a clear separation does indicate ferromagnetism in this sample. While certain contra-indications do exist, it is reasonable to conclude that Ni-implanted $\text{Al}_{0.35}\text{Ga}_{0.65}\text{N}$ does show ferromagnetism persisting to room temperature. The source of this ferromagnetism, however, may be clusters or precipitates, since experiments to determine whether preferential spin is being imparted to carriers in the semiconductor have not been performed. The most attractive feature of this material is the high M_S value and correspondingly high B_R value, which indicates the potential for enhanced magnetic stability.

4. Conclusions

The nominally undoped $\text{Al}_{0.35}\text{Ga}_{0.65}\text{N}$ samples were implanted with Cr, Mn, and Ni at room temperature with an energy of 200 keV to a dose of $5 \times 10^{16} \text{ cm}^{-2}$ for Cr and Mn and to a dose of $3 \times 10^{16} \text{ cm}^{-2}$ for Ni. Ferromagnetism for these materials that persists to room temperature after annealing under proper conditions was demonstrated through magnetic-field-dependent hysteresis loop measurements and temperature-dependent field-cooled and zero-field-cooled magnetization measurements using a SQUID magnetometer. This property is critical to the fabrication of practical spintronic devices based on dilute magnetic semiconductors. Coercive fields of 178, 180, and 195 Oe were obtained at room temperature for the $\text{Al}_{0.35}\text{Ga}_{0.65}\text{N}$ samples implanted with Cr, Mn, and Ni, respectively. The evolution of ion-implantation damage recovery was also evaluated by cathodoluminescence measurements.

The fact that the ion implantation technique can also produce dilute ferromagnetic materials with transition metal implantation enhances the capability for spintronic device fabrication if true interaction between the transition metal's d-orbital electrons and carriers in the semiconductor can be confirmed by experiments that would measure the anomalous Hall effect or magnetic circular dichroism. The results of this study will also allow AlGaN to join other wide-bandgap semiconductors in the future exploitation of room-temperature ferromagnetic semiconductors

References

- [1] T. Jungwirth, J. Sinova, J. Kuřcera, A.H. MacDonald, *Curr. Appl. Phys.* 3 (2003) 461–464.
- [2] T. Dietl, H. Ohno, F. Matsukura, J. Cibert, D. Ferrand, *Science* 287 (2000) 1019–1022.
- [3] Y. Uspenskii, E. Kulatov, H. Mariette, H. Nakayama, H. Ohta, *J. Magn. Magn. Mater.* 258–259 (2003) 248–250.
- [4] T. Dietl, *Semicond. Sci. Tech.* 17 (2002) 377–392.
- [5] C.Y. Fong, V.A. Gubanov, C. Boekema, *J. Electron Mater.* 29 (2000) 1067–1073.
- [6] R.M. Frazier, et al., *J. Appl. Phys.* 94 (2003) 4956–4960.
- [7] S.J. Pearton, et al., *J. Appl. Phys.* 93 (2003) 1–13.
- [8] S. Das Sarma, J. Fabian, X. Hu, I. Žutić, 58th Device Research Conference, IEEE, Denver, 2000, pp. 95–98.
- [9] S. Sonoda, et al., *IEEE Trans. Magn.* 38 (2002) 2859–2862.
- [10] R. Dwiliński, et al., *Diamond Relat. Mater.* 7 (1998) 1348–1350.
- [11] H. Akinaga, et al., *Appl. Phys. Lett.* 77 (2000) 4377–4379.
- [12] S. Sonoda, S. Shimizu, T. Sasaki, Y. Yamamoto, H. Hori, *Condens. Matter* 0108 (2001) 159 (available at <http://www.arxiv.org/ftp/condmat/papers/0108/0108159.pdf>).
- [13] S. Kuwabara, T. Kondo, T. Chikyow, P. Ahmet, H. Munekata, *Jpn. J. Appl. Phys., Part 2* 40 (2001) L724–L727.
- [14] N.W. Ashcroft, N.D. Mermin, *Solid State Physics*, 1st ed., Saunders College, Philadelphia, 1976.
- [15] S.J. Pearton, et al., *J. Phys.: Condens. Matter* 16 (2004) R209–R245.
- [16] M.-Y. Ryu, et al., *Phys. Status Solidi C* 0 (2003) 2593–2596

IV Summary

Ferromagnetism for Cr-, Mn, and Ni-implanted $\text{Al}_{0.35}\text{Ga}_{0.65}\text{N}$ that persists to room temperature after annealing under proper conditions was demonstrated through magnetic-field-dependent hysteresis loop measurements and temperature-dependent field-cooled and zero-field-cooled magnetization measurements using a SQUID magnetometer. This property is critical to the fabrication of practical spintronic devices based on dilute magnetic semiconductors. The fact that the ion implantation technique can also produce dilute ferromagnetic materials with transition metal implantation enhances the capability for spintronic device fabrication. However, these measurements highlight the need for further characterization to determine whether there is *sp-d* hybridization and which annealing conditions maximize true DMS behavior. In order to characterize the interaction between the transition metal's *d*-orbital electrons and carries in $\text{Al}_{0.35}\text{Ga}_{0.65}\text{N}$, magnetic circular dichroism (MCD) or X-ray MCD measurements will be performed at the AFIT or Pohang Accelerator Laboratory, respectively.